Journal of Mammalogy, 94(5):967–982, 2013

A new species of shrew-opossum (Paucituberculata: Caenolestidae) with a phylogeny of extant caenolestids

Reed Ojala-Barbour,* C. Miguel Pinto, Jorge Brito M., Luis Albuja V., Thomas E. Lee, Jr., and Bruce D. Patterson

Sección de Mastozoología del Departamento de Ciencias Biológicas, Escuela Politécnica Nacional, Casilla 17-01-2759, Quito, Ecuador (RO-B, JBM, LAV)
Department of Mammalogy and Sackler Institute for Comparative Genomics, American Museum of Natural History, Central Park West at 79th Street, New York, NY 10024, USA (CMP)
The Graduate Center, City University of New York, NY 10016, USA (CMP)
Centro de Investigación en Enfermedades Infecciosas, Pontificia Universidad Católica del Ecuador, Quito, Ecuador (CMP)
Fundación Naturaleza Kakaram, Santa Rosa 158, Bloque B y Avenida Universitaria, Quito, Ecuador (JBM)
Department of Biology, Box 27868, Abilene Christian University, 1600 Campus Court, Abilene, TX 79699-27868, USA (TEL)
Center for Integrative Research, Field Museum of Natural History, 1400 S. Lake Shore Drive, Chicago, IL 60605-2496, USA (BDP)

* *Correspondent: reed.ojala.barbour@fulbrightmail.org*

The 4 known species of northern shrew-opossums, *Caenolestes* (Paucituberculata: Caenolestidae), are restricted to the northern Andes of South America. Five specimens of a new species of *Caenolestes* were collected in Sangay National Park on the eastern slopes of the Andes in Ecuador. Review of museum specimens revealed 6 additional specimens of this species, here named *Caenolestes sangay*. All specimens were collected in cloud forest habitats from 2,050 to 3,500 m above sea level along a recently constructed highway. The new species appears to be uncommon. Inadequate sampling on the eastern slopes of the Andes limits our understanding of the distributional limits of the new species, but it occurs in a region of high endemism. New roads and land conversion threaten mature habitats near the type locality. The new species is medium sized with a narrow antorbital vacuity. It is distinguished from congeners by its large major palatine foramen and a diastema between I4 and C, among other characters. A phylogeny of Caenolestidae based on molecular and morphological characters shows a sister-group relationship between *Lestoros* and *Rhyncholestes* and indicates that the new species is likely closest to *C. caniventer*.

Key words: Andes, *Caenolestes*, cloud forest, cytochrome *b*, Eastern Versant, Ecuador, new species, phylogeny, Sangay National Park

DOI: 10.1644/13-MAMM-A-018.1

Three genera and 6 species of caenolestid marsupials comprise the extant members of the order Paucituberculata, a formerly diverse group of shrew-opossums that also includes 5 extinct families (Patterson 2008). The paucituberculatan radiation dates to the early–middle Eocene and ranged widely throughout southern South America (Goin et al. 2009). Living caenolestids are now restricted to cold and humid environments ranging discontinuously in the Andes from westernmost Venezuela to southern Chile (Patterson 2008). *Lestoros* is distributed from 2,000 to 3,600 m in southern Peru to northern Bolivia (Myers and Patton 2008), whereas *Rhyncholestes* occurs from sea level to 1,135 m in the Valdivian rain forests of southern Chile and adjacent Argentina (Patterson 2008). Each is represented by a single species.

The northern Andean genus *Caenolestes* is distinguished from other living paucituberculatans by its single-rooted, long upper canine in both sexes, P1 similar in size to P2, and I4 occupying most of the gap between I3 and C (Marshall 1980;

Albuja and Patterson 1996). An antorbital vacuity, located at the nasal, frontal, and maxillary juncture, is usually present (Albuja and Patterson 1996). The genus includes 4 species that have been informally divided into 2 species groups (Anthony 1924; Albuja and Patterson 1996; Timm and Patterson 2008). The smaller-sized, more widely distributed *C. fuliginosus* group occupies high-elevation páramo and subalpine forest, while a large-bodied group, comprised of *C. caniventer*, *C. convelatus*, and *C. condorensis*, is more restricted in range and occupies middle-elevation cloud forest and subtropical habitats. Records of *C. condorensis* are limited to the highlands of an isolated mountain range, the Cordillera del Condor (Albuja and Patterson 1996), whereas *C. convelatus* is known from the western slopes of the Andes in Colombia and northern Ecuador (Bublitz 1987). *C. caniventer* was originally described from specimens collected on the western slopes of the Andes in southern Ecuador (Anthony 1921), later recorded in northern Peru (Barkley and Whitaker 1984—as *C. fuliginosus*), and subsequently documented south of the Huancabamba Depression and on the eastern slopes of the Andes (Lunde and Pacheco 2003).

Recent distribution records reflect the inadequacy of sampling, especially at middle elevations along eastern Andean slopes, where steep, unstable slopes and extremely wet climate complicate fieldwork (Voss 2003; Patterson et al. 2012). Road construction has increased access to middle-elevation forests for scientists, but also has spurred land conversion for agriculture. In the case of Ecuador's Sangay National Park, a newly constructed highway bisected the park from Macas to Riobamba, and park forests have already been converted to cattle pasture. Mammal surveys along the newly opened highway uncovered a distinctive new shrew-opossum. Additional individuals of the new species also were identified in museum collections. Here we provide a morphological analysis and description of the new species. In addition, we provide the 1st phylogenetic hypotheses for the Caenolestidae using Bayesian analyses of mitochondrial DNA sequences and discrete morphological characters.

Materials and Methods

Study area.—We conducted our research in Sangay National Park, located on the eastern slopes of the Andes in southern Ecuador (2°13′S, 78°26′W; 517,765 ha). Trapping efforts were concentrated at a middle-elevation site (2,795 m) along a recently constructed highway that bisects the park in the Upano River valley (Supporting Information S1, DOI: 10.1644/13-MAMM-A-018.S1). Tree canopy in primary forest there reaches 25 m in height. Interior forest habitats had abundant ferns, moss, bromeliads, and orchids, whereas habitats disturbed by land-clearing and landslides supported homogenous stands of alder (*Alnus* sp.) and thickets of bamboo (*Chusquea* sp.).

Fieldwork.—Livetrapping was conducted over 15 nights, consisting of five 3-night sessions in October and November 2011, as well as March, April, and July 2012, using 100 Sherman live traps (7.5 × 9 × 27 cm; H. B. Sherman Traps, Tallahassee, Florida) and 20 Tomahawk live traps (14 × 14 × 40 cm; Tomahawk Live Trap Company, Tomahawk, Wisconsin), totaling 1,800 trap nights. Traps were set in the forest interior and along streams at 10-m intervals. Care was taken to place traps near runways, holes, and other signs of small mammal activity. Traps were baited with rolled oats, vanilla, peanut butter, and occasionally fresh trout. Procedures for handling and care of animals followed guidelines of the American Society of Mammalogists on animal care and use (Sikes et al. 2011).

Morphological terminology.—Anatomical terminology follows Wible (2003), which differs from that used in earlier caenolestid literature (e.g., Albuja and Patterson 1996) in 3 terms: incisive foramen for anterior palatal foramen, major palatine foramen for posterior palatal foramen, and postpalatine torus for palatal bridge.

Morphometrics.—Measurements follow those used in the description of *Caenolestes condorensis* (Albuja and Patterson 1996). External measures include head-and-body length (HBL), total length (ToL), tail length (TL), ear length (EL), length of the right hind foot (HF), and weight (W). HBL was determined by subtracting TL from ToL. Cranial measurements (Fig. 1) include condylobasal length (CBL), nasal length (NL), premaxillary length (PML), zygomatic breadth (ZB), mastoid breadth (MB), postorbital constriction (POC), cranial depth (CD), palatal length (PL), incisive foramen (IF), major palatine foramen (MPF), length of maxillary cheek teeth (P3M4), mandibular length (ML), and mandibular ramus height (MRH; taken from the ventral border of the ramus to the labial alveolus of m1). Dental height measurements were taken from the labial alveolus to the tip of the tooth's highest cusp. Measures include canine height (C), 1st incisor height (I1), 1st premolar height (P1), 2nd premolar height (P2), and 1st molar height (M1). Three measures of the 3rd premolar were taken: P3 height, P3 anterior style (taken along the leading edge of the tooth from the anterior alveolus to the anterior style), and P3 chordal height (taken from the anterior alveolus to the tooth crown). Dental gaps were measured from opposing alveoli of adjacent teeth. Length of the longest vibrissae was taken for each of the mystacial, superciliary, and genal fields. Measurements were taken to the nearest 0.01 mm using digital calipers and then rounded to the nearest 0.1 mm.

Morphometric analyses were conducted using Statistica (StatSoft, Inc. 2005). Ten of 11 samples of the new species were males, so morphometric analyses were limited to 85 adult males with completely erupted dentitions and closed cranial sutures, representing all recognized species of *Caenolestes* (Fig. 2). The examined specimens are listed in Appendix I. Univariate analyses employed the Basic Statistics module. Levene tests of homogeneity of variance were used to screen variables, applying a Bonferroni correction to the 18 variables examined. Because they were not recorded for many older specimens, the variables EL and W were not included in multivariate analyses, which were based on 16 variables and 74 individuals. Principal component analyses

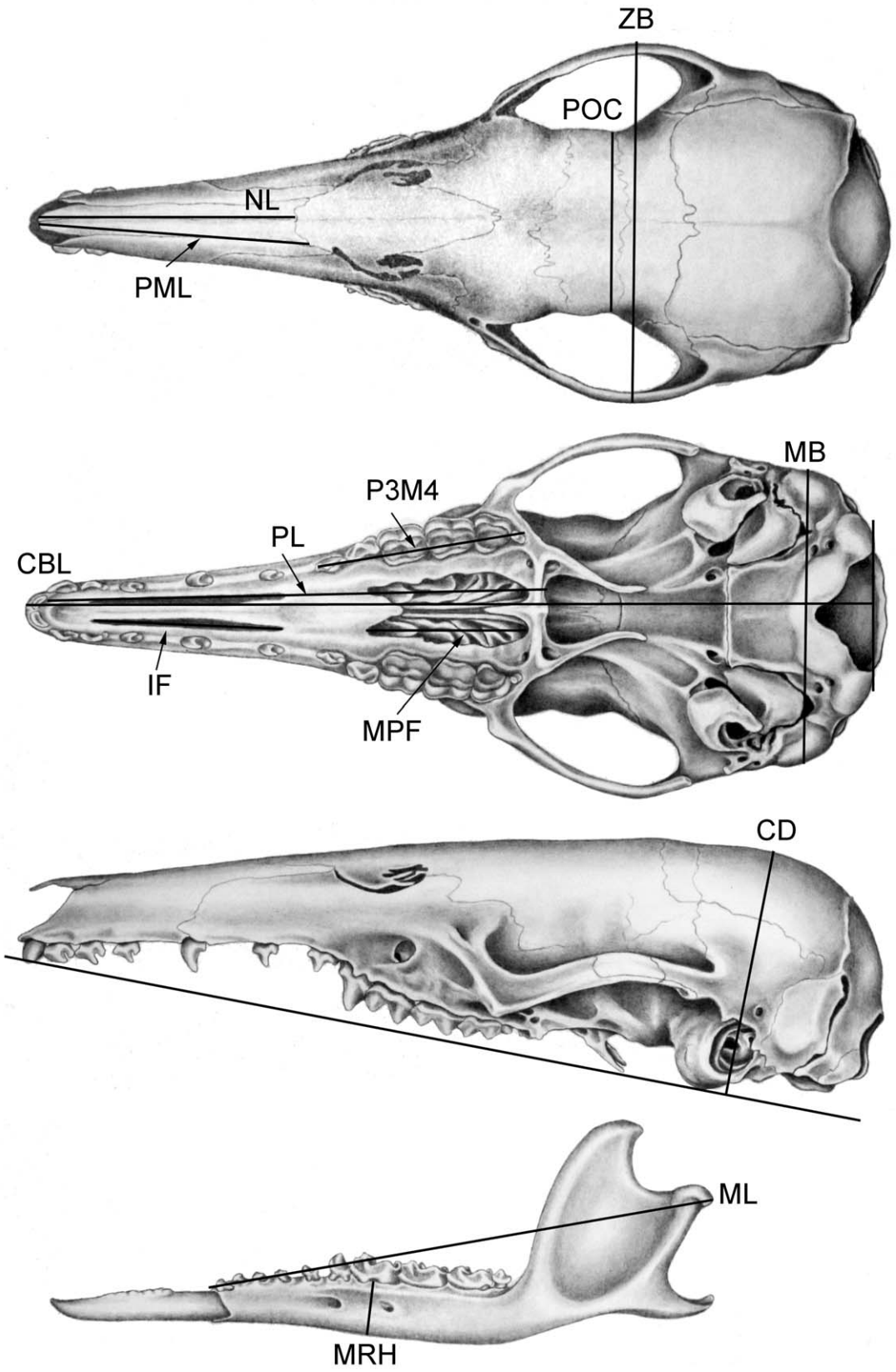

Fig. 1.—Measurements of cranial morphology taken during this study (skull drawings of *Rhyncholestes raphanurus* modified from Patterson and Gallardo [1987]): IF, incisive foramen; CBL, condylobasal length; CD, cranial depth; MB, mastoid breadth; ML, mandibular length; MRH, mandibular ramus height; NL, nasal length; P3M4, length of maxillary cheek teeth; PL, palatal length; PML, premaxillary length; POC, postorbital constriction; MPF, major palatine foramen; ZB, zygomatic breadth.

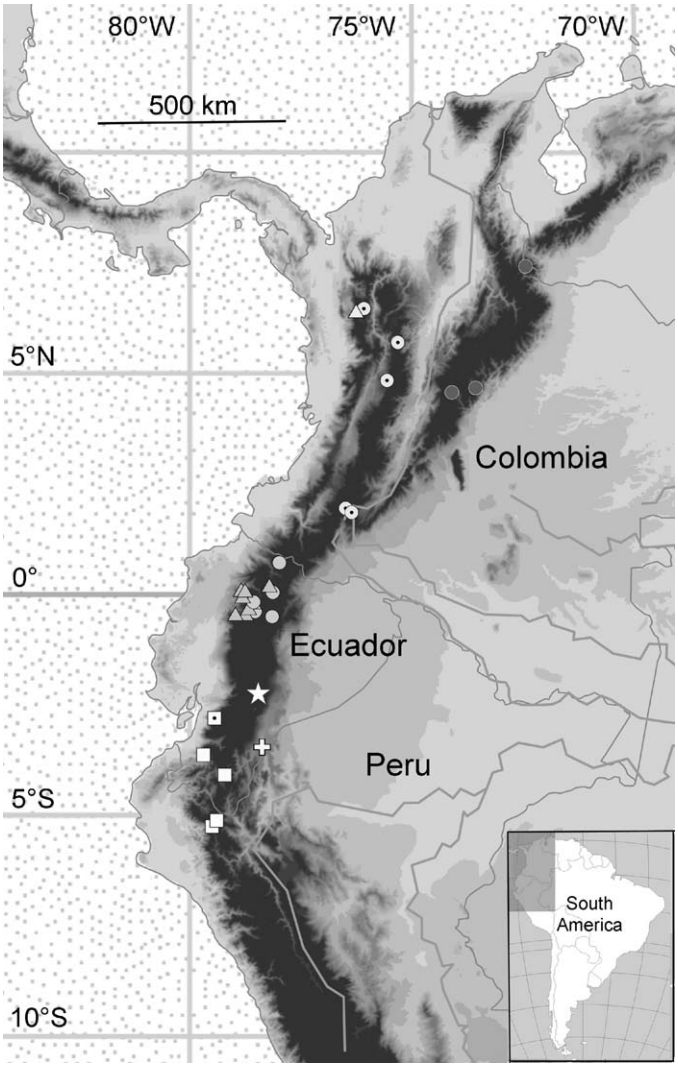

Fig. 2.—Map of *Caenolestes* specimens examined: circles, *C. fuliginosus* (pale, *C. f. fuliginosus*; dark, *C. f. centralis*; dotted, *C. f. obscurus*); triangles, C. convelatus (pale, *C. c. convelatus*; dark, *C. c. barbarensis*); squares, *C. caniventer* (dotted, type locality for *C. tatei* Anthony, 1923); plus sign, *C. condorensis*; star, the new species, *C. sangay*.

were based on the correlation matrix and included both external and craniodental characters; repeating the analyses on log-transformed craniodental characters and the covariance matrix yielded a comparable ordination of specimens. Discriminant function analyses were employed to distinguish 5 groups, the 4 recognized species of *Caenolestes* and the newly discovered one. The stepwise-addition sequence employed a *P*-to-enter-or-remove value of 0.05. Overall significance was assessed by Wilks' lambda, and distances between species' centroids in canonical space employed squared Mahalanobis distances.

Morphological data for phylogenetic analyses.—A total of 33 unordered and discrete morphological characters were scored for representatives of all extant species of the order Paucituberculata and 2 didelphid outgroups: *Metachirus nudicaudatus* and *Monodelphis domestica* (Table 1: Appendix II). The characters include external ($n = 3$) and cranial ($n = 8$) characters, and characters of both the upper ($n = 15$) and lower ($n = 7$) dentition. Descriptions follow the terminology of Wible (2003), Goin et al. (2007), and Voss and Jansa (2009). Morphological scoring and character descriptions are deposited at Morphobank at http://morphobank.org/permalink/?P762.

Tissue sampling and DNA sequencing.—Liver and muscle samples from euthanized specimens were stored in 96% ethanol and are deposited in the Instituto de Ciencias Biológicas of the Escuela Politécnica Nacional tissue collection. In addition, we received loans of tissues for *C. caniventer* (AMNH 268103, liver in ethanol), *C. condorensis* (MEPN 7463, skin snips), *C. convelatus* (QCAZ 1848, dry muscle crusts attached to skull), and *Lestoros inca* (FMNH 174481, liver in ethanol).

Total DNA extractions of the samples of *Caenolestes* n. sp., *C. caniventer*, and *L. inca* were conducted using the DNeasy blood and tissue kit (Qiagen, Valencia, California) following the fabricant instructions. For the degraded samples of *C. convelatus* and *C. condorensis*, a protocol of phenol–chloroform extraction and centrifugal dialysis was used (Fleischer et al. 2000). To avoid contamination, these DNA extractions were conducted in a room dedicated exclusively to extractions of ancient DNA in a different building from the main laboratory.

We amplified by polymerase chain reaction fragments of the mitochondrial genes cytochrome *b* (*Cytb*) and cytochrome oxidase I (COI) with illustra PuReTaq Ready-To-Go PCR beads (GE Healthcare, Little Chalfont, Buckinghanshire, United Kingdom). We amplified a fragment of 824 base pairs (bp) of the *Cytb* gene with the primers CytB1A (CCATC-

Table 1.—Matrix of scores of the 33 morphological characters (Appendix II) used in the combined phylogenetic analyses (Fig. 7b).

	1	2	3	4	5	6	7	8	9	10	11	12	13	14	15	16	17	18	19	20	21	22	23	24	25	26	27	28	29	30	31	32	33
Metachirus nudicaudatus	1	0	0	2	2	2	1	2	2	0	2	3	3	3	3	3	3	1	1	1	3	2	1	2	0	0	2	2	2	3	2	0	0
Monodelphis domestica	1	0	1	2	2	2	1	2	2	0	2	3	3	3	3	3	3	1	1	1	3	2	1	2	0	0	2	2	2	3	2	0	0
Caenolestes caniventer	1	1	0	1	1	1	0	1	0	1	1	1	1	1	1	1	1	1	1	1	1	1	1	1	1	2	1	1	1	0	1	1	1
Caenolestes condorensis	0	1	0	1	1	1	0	1	2	1	2	1	1	1	1	1	1	1	1	1	1	0	1	0	1	2	1	1	1	2	1	1	0
Caenolestes convelatus	1	0	0	1	1	1	1	0	2	0	1	1	1	1	1	1	1	1	1	1	1	1	1	0	0	1	1	1	1	2	0	0	0
Caenolestes fuliginosus	0	0	0	1	1	1	0	0	2	1	1	1	1	0	1	1	1	1	1	1	1	1	1	0	1	1	1	1	1	0	1	1	1
Caenolestes sangay	1	0	1	1	1	1	0	1	1	1	1	1	1	1	1	1	1	1	1	1	1	0	1	1	1	1	1	1	1	1	1	1	0
Lestoros inca	0	0	0	0	0	0	0	0	2	0	0	0	0	0	0	0	0	0	0	0	0	0	0	0	0	0	0	0	0	0	0	0	0
Rhyncholestes raphanurus	0	0	0	1	0	0	0	0	2	0	1	2	2	2	2	2	2	1	0	1	2	0	0	1	0	2	0	0	1	0	0	0	0

Table 2.—GenBank accession numbers of the nucleotide sequences used in this study (Fig. 7). Accession numbers in bold indicate the newly generated sequences for this study. *Cytb* = cytochrome *b*; COI = cytochrome oxidase I.

	Voucher	Reference	*Cytb*	COI
Caenolestes caniventer	AMNH 268103	This study	**KF418780**	**KF418777**
Caenolestes convelatus	QCAZ 1848	This study	**KF418782**	**–**
Caenolestes fuliginosus	—	Nilsson et al. 2003, 2004	AJ508400.1	AJ508400.1
Caenolestes sangay	MEPN 12137	This study	**KF418781**	**KF418778**
Lestoros inca	FMNH 174481	This study	**KF418779**	**KF418776**
Metachirus nudicaudatus	—	Nilsson et al. 2003	NC_006516.1	NC_006516.1
Monodelphis domestica	—	Nilsson et al. 2003	NC_006299.1	NC_006299.1
Rhyncholestes raphanurus	—	Nilsson et al. 2003, 2004	AJ508399.1	AJ508399.1

CAACATCTCAGCATGATGAAA) and CBP_1R (TGTTCGACTGGTTGGCCTCCG). For the degraded samples, we used the following primer pairs to amplify 2 fragments of 219 bp and 287 bp, respectively: CBP_132F (GGCCCACATCTGCCGAGACG) and CBP_413R (AAGGAGGTGCCAATGTAGGGGA), and CBP_541F (ACAGGATCAAACAACCCATCAGGC) and CBP_865R (GGACGAAATATTAGGCTGCGTTGTGT). For the amplification of a 606-bp fragment of the COI gene, we used the primers LCO1490 and HCO 2198 (Folmer et al. 1994). We ran all polymerase chain reactions using the touchdown polymerase chain reaction profile described by Murphy and O'Brien (2007), with a modification on the denaturation step, heating at 95°C for 5 min. We cleaned the polymerase chain reaction products with ExoSAP-IT (Affymetrix Inc., Santa Clara, California), and conducted sequencing reactions in both directions with the ABI Big Dye chemistry (Applied Biosystems, Inc., Foster City, California). For the sequencing reactions we used the polymerase chain reaction primers, and to sequence the 824-bp *Cytb* gene fragment, we used the following internal primers: CBP_1F (CGCCCACATCTGCCGAGACG) and CytB1A (CCATCCAACATCTCAGCATGATGAAA).

Molecular and combined phylogenetic analyses.—We incorporated DNA sequences available in GenBank for other representatives of the family Caenolestidae, and used sequences of the didelphimorphs *M. nudicaudatus* and *M. domestica* as outgroups (Table 2). We aligned each gene fragment independently using the Consensus Align tool in Geneious Pro version 5.6.2 (Biomatters Ltd. 2012) with default parameters (Drummond et al. 2010). We manually checked the alignment for obvious misplacements and premature stop codons. We concatenated both gene fragments using SequenceMatrix 1.7.9 (Vaidya et al. 2011) to obtain a final matrix of 1,434 bp, including 3 N sites, to ensure the same reading frame for both gene fragments. We examined the molecular data for nucleotide substitution saturation in DAMBE (Xia and Xie 2001) by plotting transitions and transversions against the genetic distances calculated using the best-fitting evolutionary model, in this case the GTR model as indicated by jModelTest (Posada 2008). Base-pair substitutions showed evidence of saturation in the asymptote of transitions in the plot (e.g., Roje 2010). Accordingly, we analyzed the amino acid version of the data set to reduce the effect of saturation of synonymous substitutions (e.g., Russo et al. 1996).

We conducted phylogenetic analyses based on molecule-only (amino acids) and combined (morphological characters + amino acid) data sets using Bayesian inference as implemented in MrBayes 3.1.2 (Ronquist and Huelsenbeck 2003). For both analyses, we used flat priors and a mixed setting of models of amino acid evolution (prset aamodelpr = mixed), where the Mtrev model outperformed other models. For the combined analysis, we also used the standard discrete model for morphological data of MrBayes. We conducted each analysis in 2 independent runs with 4 cold and 2 heated chains, sampling 100 trees every 1,000 generations. The analyses were allowed to run until reaching convergence of the runs (convergence diagnostic value, stopval, set at 0.01), which occurred at 34,000 generations in the molecular data set and at 19,000 generations in the combined data set. The first 100 trees were discarded as burn-in each analysis. Nodal support was assessed by Bayesian posterior probabilities. For comparisons with other taxa, Kimura 2-parameter genetic distances and number of differences were calculated for the nucleotide data sets of both the COI and *Cytb* genes in MEGA5.1 (Tamura et al. 2011).

Results

Morphological comparisons of the Sangay specimens with known species of *Caenolestes* clearly documented it as new (Table 3). This taxon is described here to facilitate presentation of its characteristics and discussion of its interrelationships. Quantitative and qualitative assessments of its relationships to other caenolestids follow its formal description. *Caenolestes tatei* Anthony, 1923, a subjective synonym of *C. fuliginosus* (Timm and Patterson 2008), was included in the analysis to allay possible concerns that the new species might represent this form, found in nearby Pichincha. In the following description and comparisons, the new species differs from *C. tatei* precisely in parallel with its differences from *C. fuliginosus* (see also Figs. 1–3).

Caenolestes sangay, new species

Caenolestes caniventer: Lee et al. (2011:4); not *caniventer* Anthony, 1921.

Holotype.—The holotype is a fully adult male specimen

Table 3.—Diagnostic table of comparison for *Caenolestes*.

Variable	*C. sangay*	*C. convelatus* Anthony, 1924
Size, total length (TL, adult male)	Medium, TL 241 mm	Medium, TL 253 mm
Dorsal pelage	Coarse, dark brownish gray	Coarse, dark brown
Ventral pelage	Cream to light grayish brown extending to the lips	Cream to brown, lightest at center line of venter grading to brown
Antorbital vacuity	Parenthesis or narrow comma shape bound by maxillary, nasal, and frontal bones	Crescent, parenthesis shape or closed
Dentition	Medium. Canine is medium and hooked near tip of tooth	Large. Canine is often straighter and large
Craniodental measurement (condylobasal length)	33 mm	34 mm
Palatal foramina: incisive foramen (IF); major palatine foramen (MPF)	IF: large, hooked at margins forming closed parenthesis; MPF: large, broad and very long	IF: medium, straighter, more parallel openings; MPF: medium
Distribution	Eastern slope of the Andes (Ecuador; 2,300–3,500 m)	Western slope of the Andes (Colombia, Ecuador; 2,100–3,100 m)

(MEPN 12137, field number PS8, collected on 20 October 2010 by R. Ojala-Barbour and J. Brito), prepared as a skin and skull, accompanied by stomach contents and muscle tissue preserved in 70% ethanol. A partial (801-bp) *Cytb* gene sequence from the holotype was deposited in GenBank with accession number KF418781, and a COI sequence with accession number KF418778.

Type locality.—Collected at 2,795 m on the eastern slopes of the Andes at Tinguichaca (2°13′48.72″S, 78°26′42.14″W) in Sangay National Park, Morona Santiago, Ecuador, along the Macas–Riobamba highway (see Supporting Information S1).

Paratypes.—There are 10 paratypes (9 males and 1 female). Four of these were collected at the type locality (MEPN 12134, 12136, 12147, FMNH 219794). Review of museum specimens

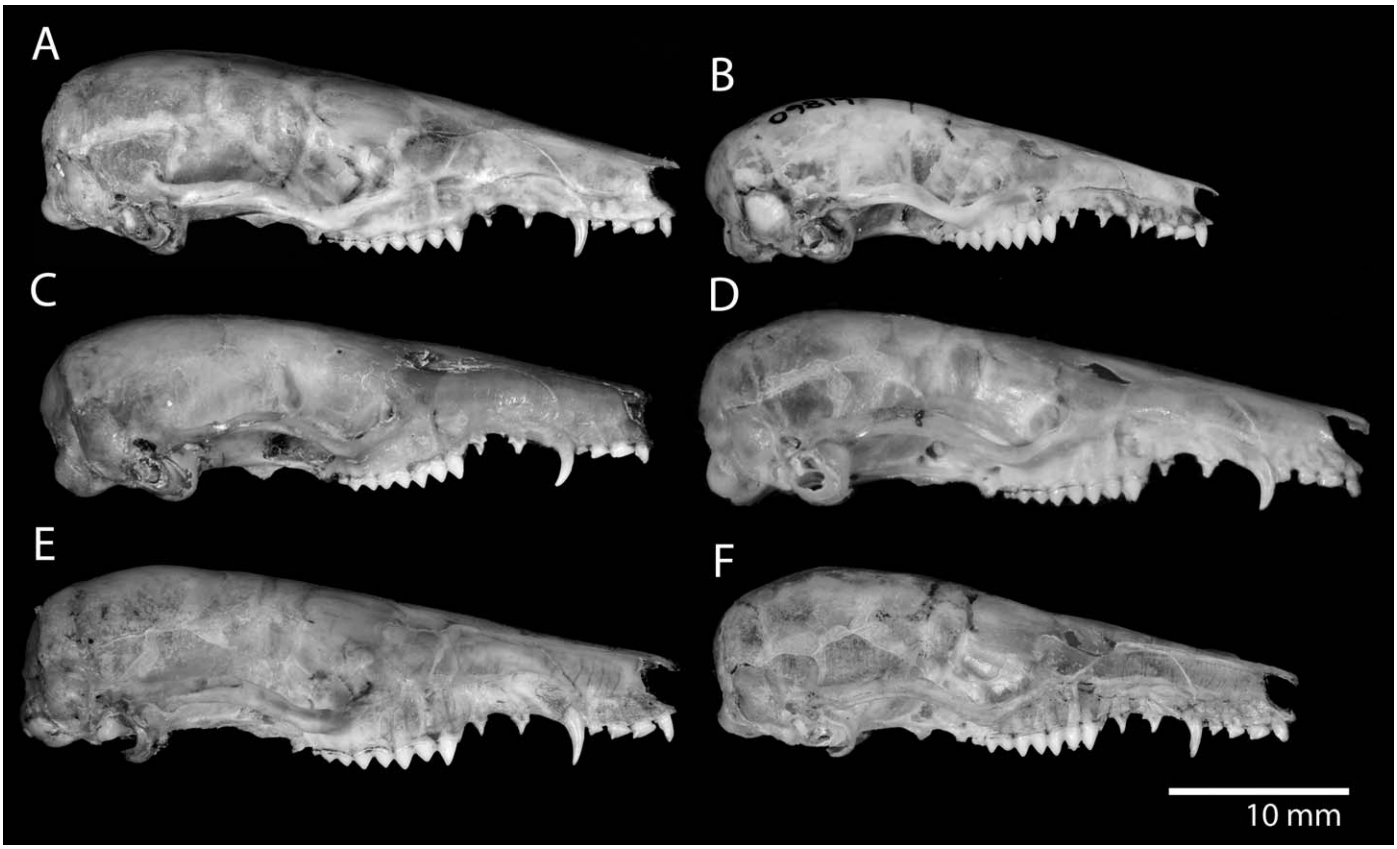

Fig. 3.—Lateral cranial views of all recognized species of *Caenolestes*. A) *C. sangay* (MEPN 12137 ♂ [holotype]); B) *C. tatei* (AMNH 61861 ♂ [holotype]); C) *C. caniventer* (AMNH 47174 ♂ [holotype]); D) *C. condorensis* (FMNH 152134 ♂ [holotype]); E) *C. convelatus* (MEPN 248 ♂); F) *C. fuliginosus* (MEPN 10628 ♂).

Table 3.—Extended.

C. caniventer Anthony, 1921	*C. condorensis* Albuja and Patterson, 1996	*C. fuliginosus* Tomes, 1863
Medium, TL 241 mm	Large, TL 261 mm	Slightly smaller, TL 237 mm
Coarse, dark brown	Coarse, dark brownish gray–fuscous	Silky, brown, little countershading
Cream colored venter, usually with dark pectoral spot	Drab brownish gray	Grayish brown, faintly contrasting with dorsal
Comma-shaped opening bound by maxillary, nasal, and frontal bones	Comma-shaped opening bound by maxillary, nasal, and frontal bones	Comma-shaped opening bound by maxillary, nasal, and frontal bones
Small to medium	Large. Canine is massive and hooked	Small. Canine small compared with relatively large incisor
33 mm	37 mm	31 mm
IF: medium, slightly hooked at margins; MPF: medium	IF: long, slightly hooked especially at anterior margin; MPF: large, massive and broad	IF: short and broad, straight or shallowly curved; MPF: small
Western slope (Ecuador; 1,600-3050 m) and eastern slope (Peru; 2,300–2,900 m) of the Andes	Cordillera del Condor, known only from type locality (Ecuador; 2,080 m)	Widely distributed at high elevations of the northern Andes (Venezuela, Colombia, Ecuador; 2,150–4,300 m)

revealed that a 5th individual (MEPN 9260) had been trapped near Zuñac along the Macas–Riobamba highway (2,050 m, 2°12′9″S, 78°24′53″W). Four additional specimens of the new species were collected 3 km up the same highway at 2,962 m (2°12′17.87″S, 78°27′30.92″W) by Lee et al. (2011): 2 deposited in the Abilene Christian University Natural History Collection (ACUNHC 1551, 1552) and 2 deposited in the Museo de Zoología at Pontificia Universidad Católica del Ecuador (QCAZ 11876, 11877). A juvenile male in the Museo Ecuatoriano de Ciencias Naturales, Ecuador (MECN 1517) was collected at the ecotone of the páramo and montane forest at 3,500 m along the same highway.

Etymology.—Parque Nacional Sangay is Ecuador's largest Andean national park, which encompasses a vast elevational gradient along the eastern slopes of the Andes and is recognized as a UNESCO World Heritage Site. The park was named after Sangay, one of Ecuador's most active volcanoes, which lies within the park's boundaries.

Diagnosis.—This is a medium-sized species distinguished externally from other species of *Caenolestes* by its grizzled brownish gray dorsum; its venter is cream-colored to pale grayish and lacks a pectoral spot. Ventral hairs are gray-based with light tips. The tail is noticeably bicolored with a very dark dorsum and warmer, drab brown venter. The tail is densely covered with short hairs that obscure the scales. The skull is medium-sized (Figs. 3A, 4A, and 5A). The antorbital vacuity is narrow to moderately open, ranging from crescent- to comma-shaped and is bounded by the maxillary and nasal bones (Fig. 4A; Supporting Information S2, DOI: 10.1644/13-MAMM-A-018.S2). The canine is medium to long, ranging from 2.7 to 3.1 mm in adult males and is slender and curved, most strongly near the tip of the tooth (Fig. 3A). The incisive foramen is slightly curved, especially at its anterior margin (Fig. 5A). The major palatine foramen is large and wide. The ventral-median lip of the foramen magnum has a U-shaped indentation between the left and right occipital condyles. The posterior margin of the postpalatine torus is curved and delicate. There is a diastema between I4 and the canine.

Description.—Externally, *C. sangay* is medium to large (Table 4). The dorsal pelage is dark grayish brown grizzled with lighter gray hairs. The ventral pelage is cream to grayish with gray-based hair and distinctly contrasts with the darker dorsum. The dorsal pelage near the midline over the lumbar vertebrae measures 14 mm. The dorsal hairs are banded, with an 11-mm gray base and grayish brown tips measuring 3 mm. Ventral hairs measure 8 mm and also are gray-based, with a 5-mm gray base tipped with 3 mm of cream. The pelage of the rostrum around the nose is darker than that of the dorsum. Just below the eyes, the pelage is cream-colored. The ears have short, well-separated hairs with the outer margins more densely covered in small, light-colored hairs. The tip of the nose, inner part of the ear, lips, and the digits of both manus and pes are rose-colored in life.

The skull is medium-sized (Table 4). The antorbital vacuity is a narrow opening in the form of a crescent or comma and is bounded by the nasal and the maxillary bones (Fig. 4A). Viewed laterally, the premaxillary extends back to the anterior margin of P3. The incisive foramen is slightly curved, especially near its anterior and posterior margins forming a closed parenthesis that extends posteriorly to the anterior margin of P2. The major palatine foramen is large and wide. The postpalatine torus is narrow and bowed, causing the anterior end of the mesopterygoid fossa to be rounded. The braincase is slightly inflated and deep. At its narrowest, the postorbital constriction is indented, with a U-shaped notch when viewed dorsally. The ventral lip of the foramen magnum is constricted at the midline by the occipital condyles, forming a moderately indented U-shape. Dorsally, the union of the occipital and the parietal forms a subtle crest. The occipital bulges to the posterior near its midpoint when viewed dorsally. The mandible is long and the ramus is delicate. The posterior margin of the angular process is slightly curved and hooked at the tip.

The species has large, long canines that are slightly curved, especially near the tip. I2–I4 are small and extend almost vertically from the alveoli. Gaps between the incisors are relatively large, especially between I1 and I2 and between I4

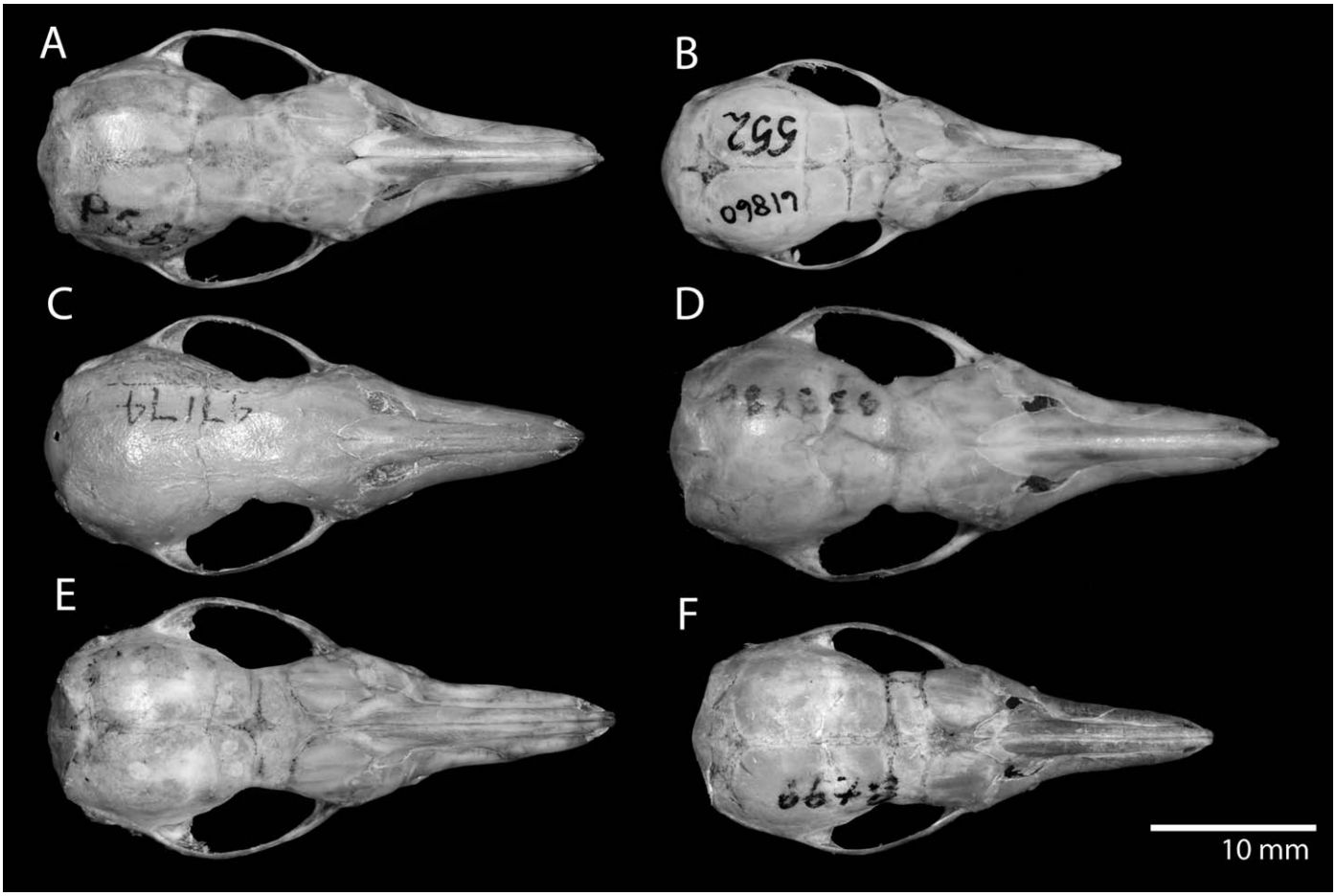

Fig. 4.—Dorsal cranial views of all recognized species of *Caenolestes*. A) *C. sangay* (MEPN 12137 ♂ [holotype]); B) *C. tatei* (AMNH 61861 ♂ [holotype]); C) *C. caniventer* (AMNH 47174 ♂ [holotype]); D) *C. condorensis* (FMNH 152134 ♂ [holotype]); E) *C. convelatus* (MEPN 248 ♂); F) *C. fuliginosus* (MEPN 10628 ♂).

and C. P1 and P2 are subequal in size. P3 is taller than the 1st cusp of M1.

Variation.—As in other species of *Caenolestes*, sexual size dimorphism is notable, with males generally larger (Albuja and Patterson 1996). The single available female skull (MEPN 12147) appears to be shorter and broader than the male skulls we examined, and its nasals are longer and mastoids broader than in most male skulls. However, its zygomatic breadth is narrower. The female has a smaller incisive foramen, but the major palatine foramen equals or is larger than in some males. The female specimen has a less pronounced occipital–parietal ridge or crest. The dentition, especially canine length, appears smaller in females.

Comparisons.—The new species lacks the dark pectoral spot that characterizes the pelage of *C. caniventer*. *C. sangay* presents a narrower, crescent- or comma-shaped antorbital vacuity (Fig. 4A), whereas that of *C. caniventer* is always comma-shaped (Fig. 4C). The major palatine foramen of *C. sangay* is larger and broader and the postpalatine torus more delicate than in *C. caniventer* (Fig. 5). The indentation of the ventral margin of the foramen magnum is shallower in *C. sangay* than the deeply notched, U-shaped constriction evident in *C. caniventer*. Viewed from above, the occipital region of the new species is more inflated at the midline than the more uniformly rounded occipital of *C. caniventer*.

From *C. convelatus*, the new species differs in that its pale gray venter extends onto the throat and chin, whereas in *C. convelatus* it terminates at the neck. The contrast between dorsal and ventral coloration in the new species is much stronger than in *C. convelatus*. The new species has a more open antorbital vacuity (Figs. 3A and 4A); in *C. convelatus*, the vacuity opens in a very narrow parenthesis or is completely roofed by bone (Fig. 4E). The new species has a longer and broader major palatine foramen. *C. sangay* has a more delicate postpalatine torus that is bowed, causing the anterior end of the mesopterygoid fossa to be rounded. The new species also has a more bowed incisive foramen, especially at the posterior and anterior margins of the foramen. The new species presents a narrower postorbital constriction, one that is abruptly indented; the postorbital constriction in *C. c. convelatus* is more uniformly narrowed, but *C. c. barbarensis* presents a stronger indentation. From *C. c. barbarensis*, the new species can be further distinguished by its smaller dentition and more gracile cranial characters. The new species has a shorter canine,

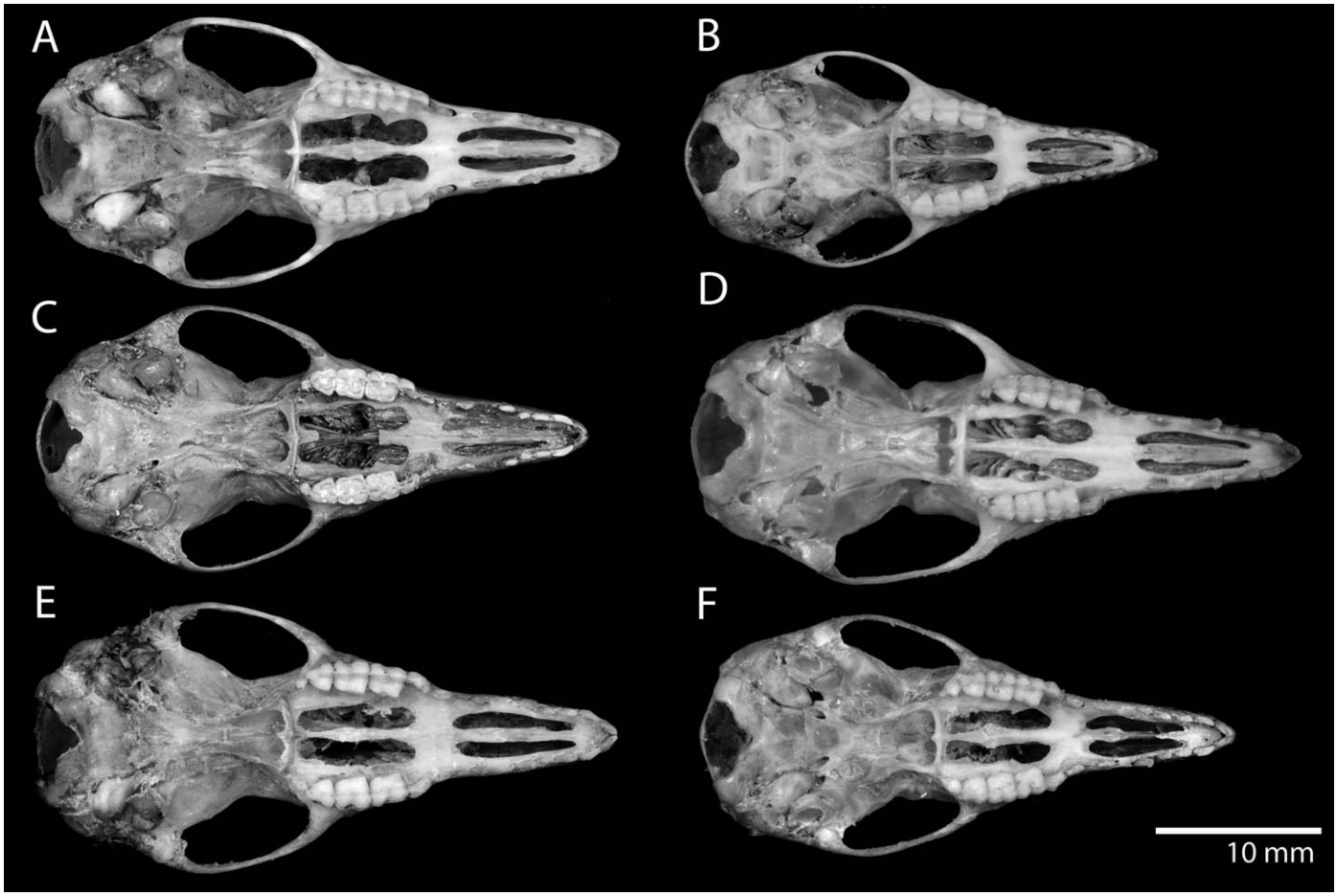

Fig. 5.—Ventral cranial views of all recognized species of *Caenolestes*. A) *C. sangay* (MEPN 12137 ♂ [holotype]); B) *C. tatei* (AMNH 61861 ♂ [holotype]); C) *C. caniventer* (AMNH 47174 ♂ [holotype]); D) *C. condorensis* (FMNH 152134 ♂ [holotype]); E) *C. convelatus* (MEPN 248 ♂); F) *C. fuliginosus* (MEPN 10628 ♂).

narrower mastoid breadth, more delicate zygomatic arches in lateral view, and a weaker parietal–occipital crest.

From *C. condorensis*, the new species is distinguished by its smaller external and cranial dimensions (Table 4). The pelage of the new species presents colder, grayish brown tones grizzled with light gray, whereas that of *C. condorensis* presents warmer browns with less grizzle. The venter of the new species is pale gray to cream, sharply contrasting with the dorsum; the venter of *C. condorensis* is more richly colored and contrasts less with the dorsum. The antorbital vacuity of the new species has a narrower opening than the large, comma-shaped vacuity of *C. condorensis* (Fig. 4D). The new species has a more curved and delicate postpalatine torus. The mandible of the new species is smaller and more delicate than that of *C. condorensis*, especially its condylar process. The angular process is more curved in the new species. The new species differs in the smaller size of the upper canine, which is straighter and more delicate in appearance than that of *C. condorensis*. The new species has a much larger gap between I4 and the canine than in *C. condorensis*, which has no gap.

From *C. fuliginosus* (and its subjective synonym, *tatei*), the new species differs in its larger craniodental and external measurements. The new species has coarse pelage, versus the more silky texture of *C. fuliginosus*. The new species has stronger dorsal–ventral countershading and its pelage is grayer than the more uniformly colored, browner pelage of *C. fuliginosus*. The tail of the new species is strongly bicolored and densely haired, not faintly bicolored and visibly scaled as in *C. fuliginosus*. The antorbital vacuity of the new species is narrower than the large, comma-shaped vacuity of *C. fuliginosus*. The new species has a larger, narrower, and more curved incisive foramen than the short, open incisive foramen of *C. fuliginosus*. The braincase of the new species appears less rounded than the deeper braincase and shorter rostrum of *C. fuliginosus*. The dentition of the new species is heavier, especially the canine.

Distribution.—Known only from the eastern slope of the Andes in southern Ecuador. All known specimens have been collected along the Riobamba–Macas highway, from 2,300 m to 3,500 m above sea level. For all localities see Supporting Information S1.

Ecology and habitat.—*Caenolestes sangay* was found in both primary and secondary upper montane cloud forest (sensu Luteyn and Churchill 2000), with abundant ferns, moss,

Table 4.—Mean values for external and craniodental measurements (mm) of adult male specimens of 5 species of *Caenolestes*, and results of 1-way analyses of variance on each of these variables. Tabulated values are means with ranges in parentheses. Sample sizes in footnotes are the minimum sample size for each series. Asterisks denote levels of statistical significance: * $P < 0.05$; *** $P < 0.001$. Measurement acronyms are defined in the "*Morphometrics*" section in the text.

	C. caniventer[a]	*C. convelatus*[b]	*C. condorensis*[c]	*C. fuliginosus*[d]	*C. sangay*[e]	*F*-test, *d.f.* = 4
External measurements						
ToL	241.2 (214–275)	253.3 (216–276)	261.5 (260–263)	237.6 (200–265)	241.2 (216–260)	3.26*
HBL	113 (91–128)	133.9 (121–146)	135 (130–140)	115.3 (96–134)	122.1 (99–137)	
TL	127.8 (118–150)	119.4 (72–131)	126.5 (123–130)	122.4 (103–139)	119.1 (95–130)	0.82
HF	25.8 (24–27)	26.8 (25–29)	28.5 (27–30)	24 (20–28)	25.2 (22–28)	8.95***
EL					15.9 (15–17)	
Cranial measurements						
CBL	32.9 (31.7–35.8)	34.8 (34.0–35.8)	36.9 (36.2–37.6)	31.6 (27.6–35.0)	33.0 (31.2–34.9)	14.8***
NL	15.8 (15.4–16.3)	17.2 (16.0–18.2)	19.1 (18.7–19.5)	14.9 (12.5–17.4)	16.0 (14.5–17.2)	20.29***
PML	10.5 (10.1–11.4)	10.7 (9.1–12.6)	12.1 (12.0–12.2)	9.7 (7.7–10.8)	11.1 (10.1–11.7)	17.87***
ZB	14.9 (14.0–16.5)	16.7 (15.7–17.5)	17.3 (17.1–17.4)	14.7 (13.2–16.2)	15.8 (14.3–17.5)	14.73***
MB	11.3 (10.9–11.9)	12.5 (11.9–13.5)	13.1 (13.1–13.1)	11.4 (10.3–12.2)	11.4 (10.9–11.9)	19.06***
POC	7.7 (7.4–8.0)	7.3 (6.7–7.9)	7.4 (7.3–7.5)	7. 5 (6.9–8.2)	7.5 (7.1–8.0)	1.49
CD	10.1 (9.7–10.4)	10.5 (10.4–10.8)	11.1 (11.1–11.1)	9.9 (9.1–10.5)	10.24 (9.9–10.5)	12.99***
ML	20.5 (19.6–22.2)	22.1 (21.4–23.2)	23.6 (23.3–24.0)	19.6 (16.4–22.4)	21.3 (20.0–22.5)	17.07***
MRH	2.5 (2.2–3.1)	3.1 (2.6–3.6)	3.0 (3.0–3.1)	2.6 (2.1–3.1)	2.6 (2.0–3.0)	8.68***
PL	17.4 (16.3–19.0)	18.6 (17.9–19.1)	19.9 (19.7–20.2)	16.7 (14.6–18.9)	18.9 (17.8–20.3)	23.19***
IF	6.3 (5.9–7.1)	6.8 (6.3–7.5)	7.0 (7.00–7.00)	6.2 (5.1–7.2)	6.6 (6.1–6.8)	9.93***
MPF	6.8 (6.3–7.5)	7.0 (6.5–7.3)	8.4 (8.1–8.7)	6.5 (5.7–7.2)	7.4 (6.9–7.6)	27.65***
P3M4	7.5 (7.2–7.7)	7.8 (6.9–8.2)	8.1 (8.1–8.1)	7.1 (6.4–7.6)	7.6 (7.3–7.9)	24.44***

[a] *Caenolestes caniventer*: external measurements, $n = 6$; cranial measurements, $n = 6$.
[b] *Caenolestes convelatus*: external measurements, $n = 11$; cranial measurements, $n = 7$.
[c] *Caenolestes condorensis*: external measurements, $n = 2$; cranial measurements, $n = 2$.
[d] *Caenolestes fuliginosus*: external measurements, $n = 55$; cranial measurements, $n = 45$.
[e] *Caenolestes sangay*: external measurements, $n = 9$; cranial measurements, $n = 9$.

bromeliads, and orchids. The new shrew-opossum was captured both on steep slopes and in level riparian forests. Other small mammal species captured at the type locality include *Thomasomys baeops*, *T. silvestris*, *Microryzomys minutus*, *Nephelomys albigularis*, and *Akodon orophilus*. Near the type locality, *A. mollis* and *T. cinnameus* also are sympatric with the new species (Lee et al. 2011). Upon capture, caenolestids appear to become trap-shy. Although 5 individuals were marked and released at the type locality, none were recaptured in 4 subsequent trapping sessions. This tendency also was noted for *C. fuliginosus* (R. Ojala-Barbour, pers. obs.) and *Rhyncholestes raphanurus* by Meserve et al. (1982).

Stomach contents.—Stomach contents of 3 preserved individuals (MEPN 12134 ♂, MEPN 12136 ♂, MEPN 12147 ♀) contained a variety of insect and plant remains, suggesting that the new species has insectivorous habits similar to those of other caenolestids (Kirsch and Waller 1979; Barkley and Whitaker 1984; Meserve et al. 1988). One individual (MEPN 12147 ♀) contained remains of a click-beetle larva (Elateridae), partial remains of an arachnid (Lycosidae), and the wings of a dipteran. Another individual (MEPN 12136 ♂) contained fragments of a wasp (Pteromalidae), an unidentified larva, bryophytes, and rhizomes. Another individual (MEPN 12134 ♂) was found with fragments of an unidentified fruit, small dark hairs, and an intact, unidentified flatworm that may have been an endoparasite.

Morphometric analysis.—Table 4 contains means and ranges of external and craniodental variables of adult male individuals of 5 species of *Caenolestes*. Also tabulated are the results of *F*-tests from 1-way analyses of variance testing for differences among species. All but 1 of the external measurements (TL) and of the craniodental characters (POC) showed significant differences among species (Table 4). Across most variables, *C. sangay* is neither the largest (often *condorensis*) nor the smallest (usually *fuliginosus*) but appears intermediate-sized. The morphometric intermediacy of *caniventer*, *convelatus*, and *sangay* is also reflected in principal components plots (not shown) showing broad overlap between species.

Nevertheless, discriminant function analysis clearly distinguishes these taxa morphometrically. In stepwise analysis, 9 variables entered the function (in order: MPF, MB, P3M4, TL, PL, CBL, HF, PML, and HBL) with individual $P < 0.05$, producing an overall function with Wilks' lambda ($F_{4,58} = 0.011$, $P < 0.0001$). Only a single individual was misclassified: 1 *fuliginosus* was classified as *caniventer*. In a plot of the first 2 canonical axes (Fig. 6), the specimens of *C. sangay* appear in a distinct cluster; in terms of squared Mahalanobis distances, their nearest neighbors are *caniventer* (32.65), followed by *convelatus* (33.08), *fuliginosus* (48.31), and *condorensis* (59.15). Nearest neighbors for other species pairs are *caniventer–fuliginosus* at 12.52, *convelatus–caniventer* at 20.18, and *convelatus–condorensis* at 35.79. Morphometric comparisons corroborate the qualitative differences that distinguish *C. sangay* from any described species of *Caenolestes*.

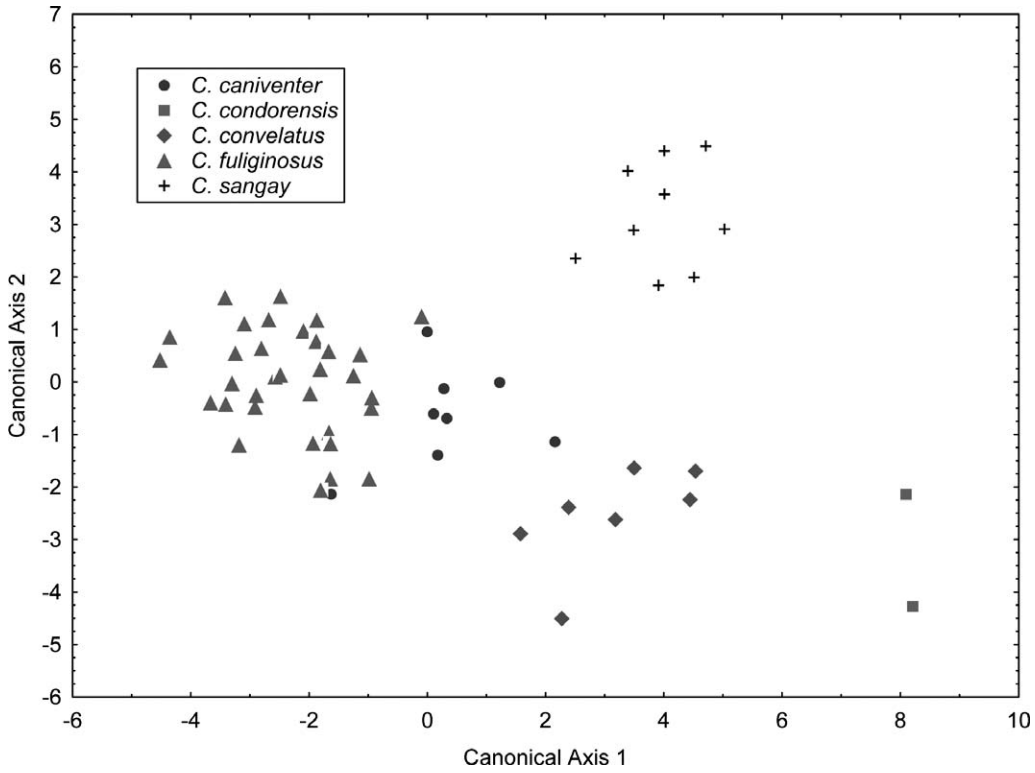

Fig. 6.—Scores on the first 2 canonical axes of discriminant function analysis of skulls of adult male *Caenolestes*: *C. caniventer* (circles), *C. condorensis* (squares), C. *convelatus* (diamonds), *C. fuliginosus* (triangles), and *C. sangay* (crosses). The overall discrimination of 5 groups was highly significant ($F_{64,154} = 5.5558$, $P < 0.00001$) and all but 1 of the samples were correctly classified (1 *C. fuliginosus* was identified by the analysis as *C. caniventer*).

Phylogenetic relationships.—We recovered genetic data for all the samples analyzed except the specimen of *C. condorensis*, producing an uneven number of species in the molecular only and combined phylogenies (Fig. 7). Both phylogenies support the monophyly of *Caenolestes*, and a sister relationship between *Lestoros* and *Rhyncholestes*. However, the combined tree has better nodal support. The basalmost species within *Caenolestes* is *C. convelatus*. The node that contains *C. sangay* is not well supported in either analysis, but this species groups with *C. condorensis* and *C.*

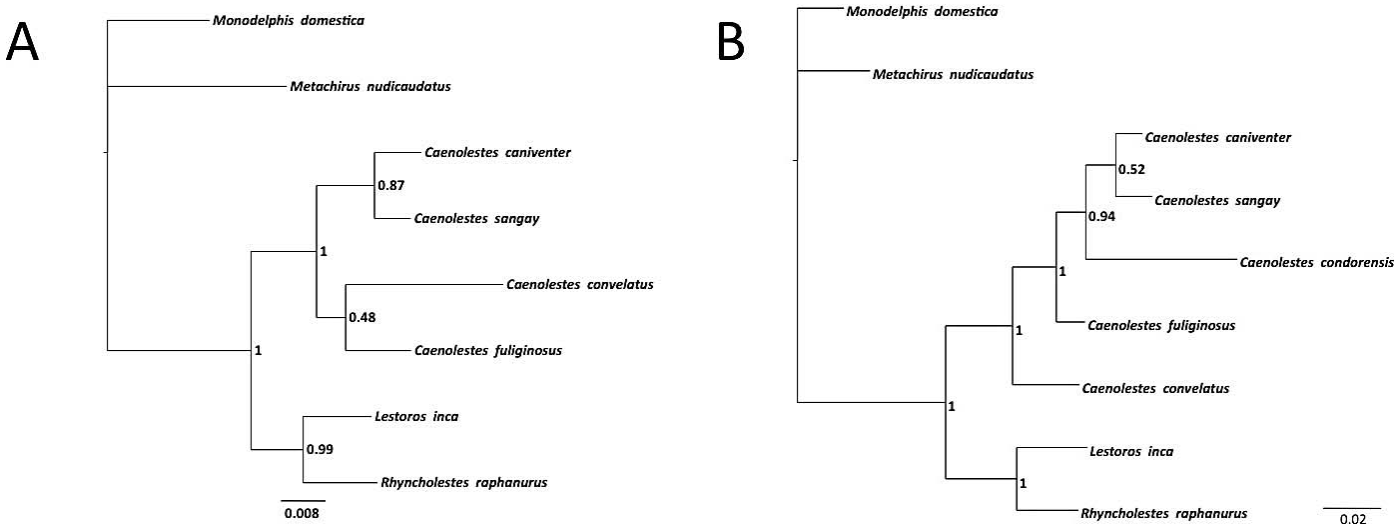

Fig. 7.—Bayesian inference phylograms of the order Paucituberculata. A) Amino acid tree depicting all extant species except *Caenolestes condorensis*. B) Combined tree of amino acids (Table 2) and 36 morphological characters (Appendix II). Numbers at the nodes are the Bayesian posterior probabilities.

Table 5.—Pairwise genetic distances of the cytochrome oxidase I gene (above the diagonal), and the cytochrome-*b* gene (below the diagonal) among the caenolestids and outgroup taxa. *K* indicates Kimura 2-parameter distances and *D* is number of differences.

	C. caniventer		*C. convelatus*		*C. fuliginosus*		*C. sangay*		*L. inca*		*M. nudicaudatus*		*M. domestica*		*R. raphanurus*	
	K	*D*	*K*	*D*	*K*	*D*	*K*	*D*	*K*	*D*	*K*	*D*	*K*	*D*	*K*	*D*
Caenolestes caniventer			—	—	0.15	81	0.07	40	0.19	101	0.23	118	0.21	112	0.19	100
Caenolestes convelatus	0.16	73			—	—	—	—	—	—	—	—	—	—	—	—
Caenolestes fuliginosus	0.16	71	0.17	75			0.15	79	0.19	101	0.20	107	0.18	98	0.17	90
Caenolestes sangay	0.09	41	0.15	68	0.17	75			0.19	102	0.23	119	0.20	104	0.18	96
Lestoros inca	0.18	81	0.19	82	0.21	90	0.18	80			0.23	118	0.19	103	0.17	90
Metachirus nudicaudatus	0.24	104	0.27	113	0.24	101	0.22	94	0.22	94			0.22	113	0.22	114
Monodelphis domestica	0.24	102	0.26	109	0.28	115	0.24	102	0.23	99	0.23	98			0.19	99
Rhyncholestes raphanurus	0.21	91	0.19	82	0.23	98	0.20	88	0.18	80	0.23	100	0.23	98		

caniventer in the combined analysis (Fig. 7B). In each analysis, the in-group taxon with the longest branch length was the species with the least data: *C. convelatus* with only 506 bp of the *Cytb* gene in the molecular analysis (Fig. 7A), and *C. condorensis* with no molecular data in the combined analysis (Fig. 7B). Nucleotide genetic distances show a high level of variation among species of caenolestids (Table 5).

Discussion

Phylogenetic relationships.—Our analyses provide the 1st phylogenetic hypothesis for all extant species of the order Paucituberculata. Despite its limited species diversity, there have been long-standing questions about the group's intergeneric and interspecific relationships.

Traditionally, *Lestoros* has been viewed as close to *Caenolestes* (Simpson 1970; Marshall 1980). Using a morphometric approach, Bublitz (1987) treated *Lestoros* as a junior synonym of *Caenolestes*. That proposal has been rejected on apomorphic grounds (e.g., Gardner 1993, 2005; Myers and Patton 2008; Timm and Patterson 2008), but until now no phylogenetic evidence has been available. Here, *Caenolestes* is recovered as a monophyletic group, and sister to the clade formed by *Lestoros* and *Rhyncholestes* (Fig. 7). This arrangement corroborates the distinction of *Lestoros* from *Caenolestes*. *Lestoros* exhibits a number of unique morphological characteristics, such as double-rooted canines and a tiny P1 (Myers and Patton 2008; Timm and Patterson 2008). Martin (2013) enumerated a host of other morphological distinctions between *Caenolestes* and *Lestoros* that confirm their status as distinct taxa.

Morphologically and geographically, the species of the genus *Caenolestes* comprise 2 groups distinguished by size and habitat: the smaller *C. fuliginosus* inhabiting upper-elevation forest and páramo environments, and the group formed by the medium- and large-sized species (*C. caniventer*, *C. condorensis*, *C. convelatus*, and now also *C. sangay*) inhabiting forested slopes at lower elevations (Anthony 1924; Albuja and Patterson 1996; Timm and Patterson 2008). Determining whether this was a natural (= monophyletic) or artificial arrangement has been impossible without a complete species-level phylogeny. Our complete phylogeny (Fig. 7B) suggests this grouping is unnatural, because the medium and large *Caenolestes* do not form a monophyletic group. However, *C. convelatus* appears as the most basal species of the genus, and unsurprisingly, it is one of the most easily differentiated caenolestids in lacking or having a much reduced antorbital vacuity (Albuja and Patterson 1996; Timm and Patterson 2008).

Additional genetic data may help to resolve the equivocal phylogenetic relationships found between *C. sangay* with *C. caniventer* and *C. condorensis*. However, we hypothesize that mountain uplift and subsequent isolation may have played an important role in the diversification of caenolestids in southeastern Ecuador. This unresolved clade is distributed discontinuously along the Andean slopes of southern Ecuador and northern Peru, and, in the case of *C. condorensis*, in the isolated Condor mountain chain east of the main cordillera.

Trapping caenolestids.—It is noteworthy that, of the various mammalian surveys of the Sangay National Park and surrounding areas (e.g., Rageot and Albuja 1994; Castro and Rivera 1999; Fonseca et al. 2003; Haynie et al. 2006; Lee et al. 2011), only Lee et al. (2011) captured *Caenolestes*. Further sampling of montane forests, especially along the eastern slopes of the Andes and isolated mountain ranges such as the Condor and Cutucú, will be necessary to elucidate the distributions and relationships of shrew-opossums. Trapping efforts in preferred habitats and with high-protein baits have revealed that caenolestids can be captured as frequently as most other sympatric small mammals (*Caenolestes*[Kirsch and Waller 1979; Lunde and Pacheco 2003], *Lestoros* [B. Patterson, pers. obs.], and *Rhyncholestes* [Patterson et al. 1989]). New road construction on montane slopes has increased access for sampling, but land conversion threatens remaining cloud forests in southeastern Ecuador.

Resumen

Las 4 especies conocidas de ratones marsupiales, *Caenolestes* (Paucituberculata: Caenolestidae), están restringidas a los hábitats asociados con los Andes del norte de América del Sur. Cinco especímenes de una nueva especie de *Caenolestes* fueron colectados en el Parque Nacional Sangay en la Cordillera Oriental de Ecuador. Una revisión de especímenes de museo reveló 6 especímenes adicionales de esta especie nueva, aquí descrita como *Caenolestes sangay*. Todos los especímenes fueron colectados en hábitats de bosque nublado

entre los 2,050 y 3,500 m sobre el nivel del mar a lo largo de una carretera recientemente construida. La nueva especie parece ser poco común. El muestreo inadecuado especialmente en la cordillera oriental limita nuestro entendimiento de los límites distribucionales de esta nueva especie, sin embrago esta es una región de alto endemismo. Nuevas vías y conversión de tierras amenazan a los hábitats que se encuentran cerca de la localidad tipo. La nueva especie es de tamaño mediano con una vacuidad anteorbital angosta. Esta especie se distingue por el tamaño grande de su foramen palatino mayor y el espacio entre el I4 y C, entre otros caracteres. Se presenta una filogenia de Caenolestidae basada en caracteres moleculares y morfológicos, mostrando una relación de grupos hermanos entre *Lestoros* y *Rhyncholestes* e indicando que la nueva especie es probablemente cercana a *C. caniventer*.

Acknowledgments

This research was funded by a Fulbright United States Student Program grant. Thanks to the Ministerio del Ambiente of Morona Santiago for permitting our research (13-2011-INVESTIGACION-B-DPMS/MAE). We extend our gratitude to Park Director, V. Leon, for providing logistical support. We thank S. Tenemaza for granting us permission to access his land. We thank W. R. Teska and Pacific Lutheran University for loaning traps and providing guidance during the study. The Barbara E. Brown Fund for Mammal Research (FMNH) funded an excursion to the Cordillera del Condor. V. Carvajal L. provided assistance with cranial images. We thank S. Burneo and A. Camacho (QCAZ) and D. Lunde and E. Westwig (AMNH) for access to specimens and tissues deposited at their institutions. We are grateful to R. S. Voss (AMNH) for comments on the morphology of Paucituberculata, K. Helgen (National Museum of Natural History) for discussions of marsupial evolution, and R. Miezio for drawing the skull in Fig. 1. CMP is grateful for the support provided by an Albert R. and Alma Shadle Fellowship in Mammalogy (American Society of Mammalogists) and Graduate Student Fellowships from the American Museum of Natural History and the Smithsonian Institution. CMP thanks R. Fleischer (National Museum of Natural History) and S. Perkins (AMNH) for hosting and supporting the molecular work at their laboratories. We all appreciate the helpful comments and suggestions made by R. S. Voss and an anonymous reviewer on a previous draft of the manuscript.

Supporting Information

Supporting Information S1.—Map of collection sites of *Caenolestes sangay*.

Found at DOI: 10.1644/13-MAMM-A-018.S1

Supporting Information S2.—Antorbital vacuity shape.

Found at DOI: 10.1644/13-MAMM-A-018.S2

Literature Cited

Albuja V., L., and B. D. Patterson. 1996. A new species of northern shrew-opossum (Paucituberculata: Caenolestidae) from the Cordillera del Condor, Ecuador. Journal of Mammalogy 77:41–53.

Anthony, H. E. 1921. Preliminary report on Ecuadorean mammals. No. 1. American Museum Novitates 20:1–6.

Anthony, H. E. 1923. Preliminary report on Ecuadorean mammals. No. 3. American Museum Novitates 55:1–14.

Anthony, H. E. 1924. Preliminary report on Ecuadorian mammals. No. 5. American Museum Novitates 120:1–3.

Barkley, J., and J. O. Whitaker, Jr. 1984. Confirmation of *Caenolestes* in Peru with information on diet. Journal of Mammalogy 65:328–330.

Biomatters Ltd. 2012. Geneious Pro version 5.6.2. Biomatters Ltd., Auckland, New Zealand.

Bublitz, J. 1987. Untersuchungen zur Systematik der Rezenten Caenolestidae Trouessart, 1898: Unter Verwendung craniometrischer Methoden. Bonner Zoologische Monographien 23:1–96.

Castro, I., and M. J. Rivera. 1999. Inventario de fauna (aves y mamíferos) del Parque Nacional Sangay. Informe Técnico Preliminar. Museo Ecuatoriano de Ciencias Naturales, Quito, Ecuador.

Drummond, A. J., et al. 2010. Geneious v5.5. http://www.geneious.com. Accessed 16 July 2012.

Fleischer, R. C., S. L. Olson, H. F. James, and A. C. Cooper. 2000. Identification of the extinct Hawaiian eagle (*Haliaeetus*) by mtDNA sequence analysis. Auk 117:1051–1056.

Folmer, O., M. Black, W. Hoeh, R. Lutz, and R. Vrijenhoek. 1994. DNA primers for amplification of mitochondrial cytochrome *c* oxidase subunit I from diverse metazoan invertebrates. Molecular Marine Biology and Biotechnology 3:294–297.

Fonseca, R. M., et al. 2003. Identificación preliminar de un corredor ecológico para mamíferos entre los parques nacionales Llanganates y Sangay. Revista de la Pontificia Universidad Católica del Ecuador 71:201–216.

Gardner, A. L. 1993. Order Paucituberculata. P. 25 in Mammal species of the world: a taxonomic and geographic reference (D. E. Wilson and D. M. Reeder, eds.). 2nd ed. Smithsonian Institution Press, Washington, D.C.

Gardner, A. L. 2005. Order Paucituberculata. Pp. 19–20 in Mammal species of the world: a taxonomic and geographic reference (D. E. Wilson and D. M. Reeder, eds.). 3rd ed. Johns Hopkins University Press, Baltimore, Maryland.

Goin, F. J., A. M. Candela, M. A. Abello, and E. V. Oliveria. 2009. Earliest South American paucituberculatans and their significance in understanding of 'pseudodiprotodont' marsupial radiations. Zoological Journal of the Linnean Society 155:867–884.

Goin, F. J., M. R. Sánchez-Villagra, A. Abello, and R. F. Kay. 2007. A new generalized paucituberculatan marsupial from the Oligocene of Bolivia and the origin of 'shrew-like' opossums. Palaeontology 50:1267–1276.

Haynie, M. L., et al. 2006. Investigations in a natural corridor between two national parks in central Ecuador: results from the Sowell Expedition, 2001. Occasional Papers, Museum of Texas Tech University 263:1–16.

Kirsch, J. A. W., and P. F. Waller. 1979. Notes on the trapping and behavior of the Caenolestidae (Marsupialia). Journal of Mammalogy 60:390–395.

Lee, T. E., Jr., C. Boada-Terán, A. M. Scott, S. F. Burneo, and J. D. Hanson. 2011. Small mammals of Sangay National Park, Chimborazo Province and Morona Santiago Province, Ecuador. Occasional Papers, Museum of Texas Tech University 305:1–14.

Lunde, D. P., and V. Pacheco. 2003. Shrew opossums (Paucituberculata: *Caenolestes*) from the Huancabamba region of east Andean Peru. Mammal Study 28:145–148.

Luteyn, J. L., and S. P. Churchill. 2000. Vegetation of the tropical Andes: an overview. Pp. 281–310 in An imperfect balance: landscape transformations in the pre-Columbian Americas (D. L. Lentz, ed.). Columbia University Press, New York.

Marshall, L. G. 1980. Systematics of the South American marsupial family Caenolestidae. Fieldiana: Geology (New Series) 5:1–145.

MARTIN, G. 2007. Dental anomalies in *Dromiciops gliroides* (Microbiotheria, Microbiotheriidae), *Caenolestes fuliginosus* and *Rhyncholestes raphanurus* (Paucituberculata, Caenolestidae). Revista Chilena de Historia Natural 80:393–406.

MARTIN, G. M. 2013. Intraspecific variability in *Lestoros inca* (Paucituberculata, Caenolestidae), with reports on dental anomalies and eruption pattern. Journal of Mammalogy 94:601–617.

MESERVE, P. L., B. K. LANG, AND B. D. PATTERSON. 1988. Trophic relationships of small mammals in a Chilean temperate rainforest. Journal of Mammalogy 69:721–730.

MESERVE, P., R. MURUA, O. LOPETEGUI N., AND J. R. RAU. 1982. Observations on the small mammal fauna of a primary temperate rain forest in southern Chile. Journal of Mammalogy 63:315–317.

MURPHY, W. J., AND S. J. O'BRIEN. 2007. Designing and optimizing comparative anchor primers for comparative gene mapping and phylogenetic inference. Nature Protocols 2:3022–3030.

MYERS, P., AND J. L. PATTON. 2008. Genus *Lestoros* Oehser, 1934. Pp. 124–126 in Mammals of South America. Vol. 1. Marsupials, xenarthrans, shrews, and bats (A. L. Gardner, ed.). University of Chicago Press, Chicago, Illinois.

NILSSON, M. A., U. ARNASON, P. B. SPENCER, AND A. JANKE. 2004. Marsupial relationships and a timeline for marsupial radiation in South Gondwana. Gene 340:189–196.

NILSSON, M. A., A. GULLBERG, A. E. SPOTORNO, U. ARNASON, AND A. JANKE. 2003. Radiation of extant marsupials after the K/T boundary: evidence from complete mitochondrial genomes. Journal of Molecular Evolution 57:S3–S12.

PATTERSON, B. D. 2008. Order Paucituberculata Ameghino, 1894. Pp. 119–120 in Mammals of South America. Vol. 1. Marsupials, xenarthrans, shrews, and bats (A. L. Gardner, ed.). University of Chicago Press, Chicago, Illinois.

PATTERSON, B. D., AND M. H. GALLARDO. 1987. *Rhyncholestes raphanurus*. Mammalian Species 286:1–5.

PATTERSON, B. D., P. L. MESERVE, AND B. K. LANG. 1989. Distribution and abundance of small mammals along an elevational transect in temperate rainforests of Chile. Journal of Mammalogy 70:67–78.

PATTERSON, B. D., S. SOLARI, AND P. M. VELAZCO. 2012. The role of the Andes in the diversification and biogeography of Neotropical mammals. Pp. 351–378 in Bones, clones, and biomes: the history and geography of Recent Neotropical mammals (B. D. Patterson and L. P. Costa, eds.). University of Chicago Press, Chicago, Illinois.

POSADA, D. 2008. jModelTest: phylogenetic model averaging. Molecular Biology and Evolution 25:1253–1256.

RAGEOT, R., AND L. ALBUJA V. 1994. Mamíferos de un sector de la alta Amazonía ecuatoriana: Mera, provincia de Pastaza. Politécnica 19:166–208.

ROJE, D. M. 2010. Incorporating molecular phylogenies with larval morphology while mitigating the effects of substitution saturation on phylogeny estimation: a new hypothesis of relationships for the flatfish family Pleuronectidae. Molecular Phylogenetics and Evolution 56:586–600.

RONQUIST, F., AND J. P. HUELSENBECK. 2003. MrBayes 3: Bayesian phylogenetic inference under mixed models. Bioinformatics 19:1572–1574.

RUSSO, C. A. M., N. TAKEZAKI, AND M. NEI. 1996. Efficiencies of different genes and different tree-building methods in recovering a known vertebrate phylogeny. Molecular Biology and Evolution 13:525–536.

SIKES, R. S., W. L. GANNON, AND THE ANIMAL CARE AND USE COMMITTEE OF THE AMERICAN SOCIETY OF MAMMALOGISTS. 2011. Guidelines for the American Society of Mammalogists for the use of wild mammals in research. Journal of Mammalogy 92:235–253.

SIMPSON, G. G. 1970. The Argyrolagidae, extinct South American marsupials. Bulletin of the Museum of Comparative Zoology 139:1–86.

STATSOFT, INC. 2005. Statistica, version 7.1. StatSoft, Inc., Tulsa, Oklahoma.

TAMURA, K., D. PETERSON, N. PETERSON, G. STECHER, M. NEI, AND S. KUMAR. 2011. MEGA5: molecular evolutionary genetics analysis using maximum likelihood, evolutionary distance, and maximum parsimony methods. Molecular Biology and Evolution 28:2731–2739.

TIMM, R. M., AND B. D. PATTERSON, 2008. Genus *Caenolestes* O. Thomas 1895. Pp. 120–124 in Mammals of South America. Vol. 1. Marsupials, xenarthrans, shrews, and bats (A. L. Gardner, ed.). University of Chicago Press, Chicago, Illinois.

TOMES, R. F. 1863. Notice of a new American form of marsupial. Proceedings of the Zoological Society of London 1863: 50–51, Pl. VIII.

VAIDYA, G., D. J. LOHMAN, AND R. MEIER. 2011. SequenceMatrix: concatenation software for the fast assembly of multi-gene datasets with character set and codon information. Cladistics 27:171–180.

VOSS, R. S. 2003. A new species of *Thomasomys* (Rodentia: Muridae) from eastern Ecuador, with remarks on mammalian diversity and biogeography in the Cordillera Oriental. American Museum Novitates 3421:1–47.

VOSS, R. S., AND S. A. JANSA. 2009. Phylogenetic relationships and classification of didelphid marsupials, an extant radiation of New World metatherian mammals. Bulletin of the American Museum of Natural History 322:1–177.

WIBLE, J. R. 2003. On the cranial osteology of the short-tailed opossum *Monodelphis brevicaudata* (Didelphidae, Marsupialia). Annals of Carnegie Museum 72:137–202.

XIA, X., AND Z. XIE. 2001. DAMBE: data analysis in molecular biology and evolution. Journal of Heredity 92:371–373.

Submitted 7 January 2013. Accepted 29 May 2013.

Associate Editor was Ryan W. Norris.

APPENDIX I

Specimens examined.—Acronyms for institutions housing recent mammal collections used in the analyses are as follows: Abilene Christian University Natural History Collection (ACUNHC); American Museum of Natural History (AMNH); Escuela Politécnica Nacional, Ecuador (MEPN); Field Museum of Natural History (FMNH); Museo Ecuatoriano de Ciencias Naturales, Ecuador (MECN); Museum of Zoology of Louisiana State University (LSUMZ); and Pontificia Universidad Católica del Ecuador, Ecuador (QCAZ). The museum numbers of specimens used in the morphometric analyses shown in italics. A subjective synonym of *Caenolestes fuliginosus*, *Caenolestes tatei* Anthony 1923, is included in our comparisons because of its geographic distribution, which is close to the type locality of *C. sangay*. Further taxonomic work is needed to clarify the status of *tatei*.

Caenolestes caniventer.—**Ecuador**: El Oro; El Chiral, 5,350 feet [1,630 m] (*AMNH 47170* ♂, *47173* ♂, 47174 ♂ [holotype], *47175* ♂); Loja; Lago El Compadre, Cajanuma, 2,525 m (MEPN 244 ♂). **Peru**: Piura; Cerro Chinguela, approximately 5 km N Sapalache,

2,900 m (*LSUMZ 25389* ♂, *25391* ♂, *25393* ♂); Huancabamba, 3,000 m (FMNH 81456–81458 ♀, 81460 ♂, 81461–81464 ♀).

Caenolestes condorensis.—**Ecuador**: Morona-Santiago; Achupallas, 2,100 m (*FMNH 152134* ♂ [holotype], *MEPN 933875* ♂, 933874 ♀ [paratypes]).

Caenolestes convelatus barbarensis.—**Colombia**: Antioquia; Santa Barbara, 2,700 m (*FMNH 70893* ♂); 3,000 m (*FMNH 70894* ♂, *70906* ♂); 2,800 m (*FMNH 70891* ♂, *70892* ♂, 70895 ♀, 70896 ♀, 70898 ♀, 70899 ♀, 70907 ♀).

Caenolestes convelatus convelatus.—**Ecuador**: Imbabura; Hacienda La Vega, 5 km ESE San Pedro del Lago (*FMNH 124620* ♂); Pichincha; Las Maquinas, Santo Domingo Trail, 7,000 feet [2,134 m] (*AMNH 64456–64458* ♂, *64461* ♂); Santa Rosa, Mindo (*MEPN 59* ♂); El Palmito, 2,300 m (MEPN 248 ♂); Saloya West, 1,100 m (FMNH 53288 ♀), Ilambo Valley, 1,800 m (FMNH 94948 ♂); Cotopaxi; Reserva Otonga, 1,800 m (QCAZ 1789 ♂, 1792 ♂, 1798 ♂, 1847 ♂, 1848 ♀, 3166 ♂); Esmeraldes; El Castillo (FMNH 44319 ♀).

Caenolestes fuliginosus centralis.—**Colombia**: Antioquia; Páramo Frontino, 3,300 m (*FMNH 70836–70838* ♂); Páramo, 7 km E, 3,000 m (*FMNH 69820* ♂); 3,050 m (*FMNH 70543* ♂); 3,100 m (*FMNH 70544* ♂); Caldas; Rio Termales (*FMNH 70825* ♂); 2,600 m (*FMNH 70831* ♂, *70834* ♂); 3,100 m (*FMNH 70833* ♂, 70839 ♀, 70545 ♀, 69821 ♀, 69820 ♀); 3,200 m (*FMNH 70827* ♂); 3,300 m (*FMNH 70823* ♂, *70835* ♂); Huila; Rio Magdalena, 2,200 m (*FMNH 70842* ♂, *70843* ♂); 2,300 m (*FMNH 70841* ♂, *70847–70849* ♂); Rio Ovejeras, 2,350 m (*FMNH 70844* ♂).

Caenolestes fuliginosus fuliginosus.—**Ecuador**: Napo; Cerro Antisana, oriente (*FMNH 43164* ♂); Pichincha; Chinchin Cocha, 4,000 m (*FMNH 53289–53292* ♂, *53294* ♂); Molleturo, 7,600 feet [2,316 m] (*AMNH 61861* ♂ [holotype of *C. tatei* Anthony, 1923]); Mt. Pichincha, San Ignacio, 4,000 m (*AMNH 64372* ♂, *64375* ♂, *64376* ♂, *64379* ♂, *FMNH 53296* ♂, *53299* ♂); 3,300 m (*FMNH 53298* ♂); 3,800 m (*FMNH 53300* ♂); 4,200 m (*FMNH 53302* ♂, *53303* ♂); Carchi; El Espejo, El Angel, 3,630 m (MEPN 10484 ♂, 10888 ♀, 10628 ♀, 10881 ♂).

Caenolestes fuliginosus obscurus.—**Colombia**: Cundinamarca; Rio Balcones (*FMNH 70860–70862* ♂); 2,700 m (*FMNH 70863–70868* ♂, *70870* ♂); San Cristobal, 2,900 m (*FMNH 70876–70878* ♂, *70881*♂, *70880* ♂, 70882 ♀, 70887 ♀, 70886 ♀); Norte de Santander; Páramo de Tama, 3,329 m (*FMNH 18599* ♂, *18603* ♂).

Caenolestes sangay.—**Ecuador**: Morona Santiago, Zuñac, Tinguichaca, 2,962 m (*ACUNHC 1551* ♂, *1552* ♂, *QCAZ 11876* ♂, *11877* ♂); 2,795 m (*MEPN 12134* ♂, *12136* ♂, *12137* ♂ [holotype], *FMNH 219794* ♂, MEPN 12147 ♀); 2,050 m (*MEPN 9260* ♂).

Lestoros inca.—**Peru**: Cusco; Paucartambo, La Esperanza, 2,880 m (FMNH 174477 ♀, 174481 ♂, 174483 ♂).

Rhyncholestes raphanurus.—**Chile**: Los Lagos; Osorno, Valle de la Picada, La Picada, Refugio, 820 m (FMNH 50071 ♂); La Picada Alto, 595 m (FMNH 129823 ♂); La Picada Alto, 600 m (FMNH 129830 ♀).

Metachirus nudicaudatus.—**Peru**: Cusco; Paucartambo, Consuelo, 15.9 km SW Pilcopata, 1,000 m (FMNH 174441 ♂).

Monodelphis domestica.—**Paraguay**: Boqueron, Filadelfia, 35 km W Estancia Toledo–Toledo (FMNH 164090 ♀, 164091 ♂).

Appendix II

List of morphological characters scored for all living species of Caenolestidae, and 2 didelphid outgroups, used in the combined phylogenetic analysis (Fig. 7B). Anatomical terms follow Wible (2003), Goin et al. (2007), and Voss and Jansa (2009). We consistently employ major palatine foramen (Wible 2003), rather than maxillopalatine fenestra (Voss and Jansa 2009).

External morphology

1. Skin, countershade between ventral and dorsal region: absent (0); present (1).
2. Presence of chest spots: absent (0); present (1).
3. Tail: with sparse hair, scales are visible (0), with dense hair, scales not visible (1).

Skull

4. Mediolateral alignment of minor palatine foramen and sphenopalatine foramen: aligned in mediolaterally straight line (0); sphenopalatine foramen located slightly more anterior than posterolateral palatal foramen (1); sphenopalatine foramen located significantly more anterior than posterolateral palatal foramen (2).
5. Suprameatal foramen: small and rounded (0); larger and irregularly shaped (1); larger and rounded (2).
6. Opening of infraorbital foramen: visible in lateral view (0); not visible in lateral view, concealed by the maxillary bone (1); not seen in lateral view, covered by the maxillary bone, forming a more elongated and robust channel than in 1 (0).
7. Antorbital vacuity: well-developed (0); absent, or very reduced (1).
8. Lateral margin and relative size of the incisive foramen: long and straight (0); long and curved (1); short and curved or irregular (2).
9. Notch in the midline of the ventral margin of the foramen magnum: pronounced and rounded (0); pronounced and notch tip expanded forming a ratchet-like cavity (1); shallow notch (2).
10. Postorbital constriction: uniformly smooth (0); abruptly indented with a U-shape notch at its narrowest point (1).
11. Retromolar foramen in the mandible: large and rounded (0); small and irregular (1); highly reduced or absent (2).

Upper dentition

12. Posteriormost cusp on I2: absent (0); present as a small cusp (1); present as a large, rounded cusp (2); present as a large, pointed cusp (3).
13. Ventral margin of I2: straight with no notch (0); straight with a notch (1); no notch, with curved cusps (2); no notch, large, straight, prominent cusp (3).
14. Posteriormost cusp on I3: absent (0); present as a small cusp (1); present as a large, rounded cusp (2); present as a large, pointed cusp (3).
15. Ventral margin of I3: straight with no notch (0); straight with a notch (1); no notch, with curved cusps (2); no notch, large, straight, prominent cusp (3).

16. I4: gracile tooth with a single pointed cusp (0); having a flat ventral margin with no prominent cusp present, or with the posteriormost corner of the ventral margin resembling a cusp (1); with 3 pointed crowns, the middle of which is the most prominent (2); robust tooth with a single cusp (3).
17. Diastema between upper canine and I4: moderate (0); absent or very reduced (1); large (2); pronounced with a rounded edge in the maxilla (3).
18. C in males: with 2 roots (0); with a single root (1).
19. C: small, so that skulls rest on the bullae and incisors when placed on a flat surface (0); large, so that skulls rest on canines and bullae when placed on a flat surface (1).
20. P1: reduced (0); well developed (1).
21. P2: enlarged posteriorly, with a single cusp (0); not enlarged posteriorly, with 3 cusps present, namely a large central cusp and 1 anterior and 1 posterior accessory cusp (1); enlarged posteriorly, with 3 cusps present, namely a large central cusp and 1 anterior and 1 posterior accessory cusp (2); robust, not enlarged posteriorly, with 1 central cusp and tiny anterior and posterior accessory cusps (3).
22. M1 with hypoflexus between protocone and metaconule on lingual side: imperceptible (0); modest or well developed (1); hypoflexus and metaconule both absent (2).
23. M2 with neomorphic labial cingulum at the anterior end of ectoflexus: present (0); absent (1).
24. M3 metaconule: reduced (0); expanded (1); absent or very reduced (2).
25. M4 neomorphic cingulum labial to stylar cusp B: absent (0); present (1).
26. M4 with valley on crown: absent (0); 1 well pronounced (1); 2 valleys with associated extra cusp (2).

Lower dentition

27. i1: procumbent and large, with a distinct shovel-shape (0); procumbent and large, but not shovel-shaped (1); nonprocumbent and relatively small (2).
28. i2 (the tooth immediately posterior to i1, following Martin [2007]): procumbent, larger than more posterior unicuspids (0); procumbent, smaller or roughly the same size as more posterior unicuspids (1); nonprocumbent (2).
29. m3 with elevation of metaconid and entoconid as seen in lingual view: slightly elevated (0); greatly elevated (1); elevated but height of entoconid smaller than metaconid (2).
30. m4 with paraconid as seen in lingual view: developed (0); slightly developed (1); absent (2); joined to paracristid (3).
31. m4 with labial cingulid: small (0); well developed (1); absent (2).
32. m4 entoconid forming a distinctive, rounded lobe: absent (0); present (1).
33. m4 preentocristid: contacts metaconid (0); does not contact metaconid (1).